In Situ Atomic Force Microscopy Imaging of Adsorbed Block Copolymer Micelles

Ian W. Hamley,*,‡ Simon D. Connell,† and Stephen Collins‡

Department of Chemistry and Department of Physics and Astronomy, University of Leeds, Leeds LS2 9JT, UK

Received March 26, 2004; Revised Manuscript Received May 5, 2004

ABSTRACT: Atomic force microscopy has been used to study the in situ adsorption of an amphiphilic block copolymer from aqueous solution onto hydrophilic mica and hydrophobic silica substrates. Adsorption was studied as a function of concentration—close to and below the bulk critical micelle concentration the copolymers adsorb as single chains or "premicelle aggregates". As concentration is increased, micelles form into densely packed structures. At a given concentration, the ordering is higher for the strongly adsorbed micelles on silica. Competitive adsorption onto the hydrophilic silicon nitride AFM tip occurs. The substrate coverage of micelles on mica increases roughly linearly with scan time at low micelle concentration. Weak adsorption on mica was analyzed to provide a two-dimensional diffusion coefficient. The effect of tip oscillation frequency on the AFM images was investigated—higher frequencies were required to image polymer aggregates on mica. Finally, force−distance curves provide information on the nanomechanical properties of the adsorbed polymer layers. Evidence is presented to show that micelles and aggregates adsorb to silica via the hydrophobic P block, while they adsorb to mica via the hydrophilic E block.

1. Introduction

The adsorption of surfactants and copolymers onto solid substrates is relevant to their use in applications including detergency, oil recovery, and lubrication.[1,2] Under appropriate conditions, it is possible for adsorption of micelles to occur, rather than single chains. This provides a route, for example, for the controlled deposition of inorganic nanoparticles, prepared from precursors (such as metal salts) sequestered within the micellar core.[3,4] The structure of block copolymer micelles on solid substrates has been probed on dried films by atomic force microscopy.[4−6] In addition, transmission electron microscopy can be used to image specimens that have been suitably cryo-cooled (sometimes the specimens are also stained to enhance contrast).[5,7−12]

Eisenberg and co-workers have imaged surface micelles formed by amphiphilic diblocks deposited by the Langmuir−Blodgett technique at the air−water interface.[13−15] The films were picked up onto supported TEM grids, then dried, and shadowed with metal vapor before examination by TEM. The same group has also performed AFM on dried micelles on glass.[16] Meiners et al.[17] and Spatz et al.[4,5] have observed surface micelles of polystyrene-*b*-poly(2-vinylpyridine) (SV) diblocks on mica or carbon. Samples were prepared by drying dip-coated films of diblocks (dissolved in toluene), vitrification on solvent evaporation leading to trapping of micellar structures. Regenbrecht et al.[18] probed the structure of micelles of the neutral-polyelectrolyte diblock copolymer poly(ethylethylene)-*b*-poly(styrenesulfonic acid) adsorbed on solid substrates in aqueous solution by AFM on dried samples. A comparison was made between adsorption onto a neutral hydrophobic graphite substrate and onto mica modified to be positively charged by a coating of poly(ethylenimine) or by ion exchange. They observed a range of structures from spherical micelles to network-like structures by varying ionic strength. These authors also reported that strongly charged substrates led to the formation of structures not found in the bulk.[6,18]

There have been surprisingly few AFM studies of the structure of "wet" adsorbed block copolymer micelles. Webber et al.[19] investigated the adsorption of poly(2-(dimethylamino)ethyl methacrylate)-*b*-poly(methyl methacrylate) (PDMA-*b*-PMMA) onto mica as a function of pH via in situ AFM. They observed surface micelles at low pH and regions of close-packed structure at higher pH for this polyelectrolyte diblock. Subsequently, they have observed hexagonal close-packed structures in an adsorbed layer of a related diblock, PDMA-*b*-poly(2-(diethylamino)ethyl methacrylate), in which the PDMA block was 10% quaternized.[20] The structure of the polymer layer was influenced by the electrostatic interaction between the PDMA block and the negatively charged mica.

There has been much controversy concerning the correlation between the formation of surface micelles and the bulk critical micelle concentration (cmc). Surface plasmon resonance experiments revealed a correlation between the rate of adsorption of SV diblocks from toluene and the bulk cmc—the initial rate of adsorption increasing above this concentration.[21] According to Tassin et al., the adsorbed surface micelles act as a barrier that slows down the subsequent adsorption of unimers, observed as an additional slow process. The increase in adsorption rate is due to adsorption of micelles. A study of the adsorption kinetics of polystyrene−poly(ethylene oxide) diblock copolymers onto dielectric substrates (glass and sapphire) using optical interferometry provided evidence for the adsorption of micelles above the cmc.[22] The adsorbed amount increased steeply up to the cmc; however, it then decreased sharply, and a slower increase was observed at higher concentration. The rate of adsorption also showed

† Department of Physics and Astronomy.
‡ Department of Chemistry.
* Author for correspondence.

10.1021/ma049396f CCC: $27.50
Published on Web 06/15/2004

a discontinuity at the cmc. The adsorption of other types of poly(ethylene oxide) (E)-containing block copolymers has also been investigated.[23−27] Ellipsometry on EPE (P = poly(propylene oxide)) copolymers (trade name Pluronic) adsorbed onto a hydrophilic silicon surface provided evidence for an increase in adsorbed amount just below the bulk cmc, although this effect was not noted on a hydrophobic treated silica surface.[23] It was proposed that surface association occurred on silica, in particular because the increase in adsorbed amount occurred cooperatively, but since the adsorbed layer was susbstantially less thick than the hydrodynamic radius, adsorption of intact micelles did not occur. It was concluded that the hydrophilic E block, rather than the hydrophobic P block, has the stronger tendency to adsorb,[23] an observation which we consider in our interpretation below of AFM images showing adsorbed surface micelles formed by related EP diblocks. For ETE (T = polytetrahydrofuran) and EPE copolymers, Tiberg and co-workers found that the amount of adsorbed copolymer increases 2 orders of magnitude below the cmc for the ETE copolymers and close to the cmc for the EPE triblocks.[24] This increase was related to the cooperative formation of surface micellar structures on hydrophilic surfaces. In contrast, at hydrophobic surfaces, monolayers were observed. AFM on related alcohol exthoxylate surfactants CE (C = polymethyl) provided direct evidence for the formation of surface micelles on a hydrophilic substrate and a monolayer on a hydrophobic substrate.[25] Measurements using the surface forces apparatus on an ETE triblock also provided evidence for short-range attractions between surface aggregates due to bridging of the gap between hydrophilic quartz surfaces.[28] Muller and co-workers reported no correlation between the adsorption of EL (L = polylactide) diblocks onto hydrophilic silica and micellization in bulk.[26] By comparing the adsorption of the diblock and that of E homopolymer, it was found that the hydrophobic block drives adsorption (in contrast to the conclusions of Malmsten et al. on EPE triblocks[23]). On hydrophobized silica, the same diblocks formed a monolayer, anchored by the adsorbed L blocks.[27]

The adsorption of block copolymers onto solid substrates has been investigated extensively by lattice self-consistent mean-field calculations.[29,30] These models consider adsorption of polymer chains, rather than micelles, and properties such as surface density, segment density profiles, and adsorbed layer thickness can be calculated. Zhan and Mattice performed lattice Monte Carlo simulations of adsorption of model $A_{10}B_{10}$ diblocks in a selective solvent for A.[31,32] They found that, below and close to the cmc, adsorption of free chains only occurs. In contrast, at concentrations much higher than the cmc, adsorption of micelles predominates.[32] They were able to reproduce the observations of Munch and Gast concerning the adsorbed amount (Γ) as a function of concentration—in particular, a linear increase in Γ below the cmc, followed by a drop to a lower adsorbed amount above the cmc (only weakly dependent on concentration). At a concentration about 10 times the cmc, the adsorption of micelles was marked by an increase in the concentration dependence of adsorbed polymer.[32] This regime was not encountered by Munch and Gast, who suggest adsorption of micelles commences at the cmc. Zhan and Mattice suggest that the increased adsorption rate above the cmc observed by Munch and Gast can be interpreted as arising from collisions of micelles with the surface, which do not subsequently adsorb. Johner and Joanny have suggested that even from a micellar solution, only free chains adsorb, and never complete micelles, due to the potential barrier for micellar adsorption.[33] On the other hand, the formation of surface micelles by adsorption of diblocks at a solid surface from a selective solvent has been predicted on the basis of a modified "brush" theory.[34] The result of Johner and Joanny also seems to be contradicted by experiment.

Adsorption of a series of EPE (Pluronic) copolymers onto model hydrophobic self-assembled monolayer surfaces has been studied by AFM and surface plasmon resonance (SPR).[35] Adsorption isotherms were obtained from SPR, and the adsorbed amount was found to go through a maximum near the cmc, contrary to the Langmuir isotherm. The adsorption process was found to be partly irreversible. Surface micelle structures were only observed (by AFM) for the more hydrophobic copolymers, the more hydrophilic ones adsorbing as unimers to form a uniform layer. Force−distance curves suggested a brushlike structure of adsorbed micelles. The surface structure was shown to depend on the tip force applied. It was suggested that higher force scans revealed the micellar core structure, in contrast to low force scans which probed the polymer brush coronas. In a sister paper,[36] the kinetics of adsorption was analyzed by SPR. Enhanced adsorption rates for more hydrophobic triblocks was observed above the cmc due to adsorption of micelles. Adsorption of unimers was inferred for more hydrophilic copolymers.

In the present paper, we describe experiments using AFM to image the structure of neutral diblock copolymer micelles adsorbed onto hydrophobic and hydrophilic substrates in aqueous solution. Using a custom synthesized PE diblock enables the study of adsorption without the influence of chain architecture (bridging or looping) observed for commercially available EPE (or PEP) Pluronics. The adsorbed structure on both hydrophobic silica and hydrophilic mica is compared and studied as a function of copolymer concentration. For weakly adsorbed micelles on mica, it was possible to analyze micelle motion, providing a two-dimensional diffusion coefficient. Force−distance curves were also obtained, and these provide additional insights into the packing of the adsorbed copolymer chains, in micelles at high concentration or as nonassociated "brush" chains at lower density. In a previous note,[37] we have presented a brief account of AFM results on adsorption onto silica alone.

2. Experimental Section

The copolymer $P_{94}E_{316}$ (the subscripts indicate the number of repeats) was prepared by sequential anionic polymerization of propylene oxide followed by ethylene oxide.[38] The polymer has a narrow molecular weight distribution, $M_w/M_n = 1.07$. Micellar properties in bulk solutions, including the thermodynamic and hydrodynamic radius from static and dynamic light scattering, and critical micelle temperature/concentration have been reported previously.[38]

Spontaneous adsorption of $P_{94}E_{316}$ diblock copolymer micelles from solutions of varying concentration (0.1−2.0 wt % in Milli-Q water) was studied. A MultiMode AFM with a Nanoscope IIIa controller (Veeco Instruments Ltd., Santa Barbara, CA) was used for in-situ imaging of the adsorbed layer. The fluid cell was cleaned with a 0.5% solution of Micro-90 (International Products Corp., Burlington, NJ) in Milli-Q water and thoroughly rinsed before use. Oxide-sharpened silicon nitride cantilevers (NP-S, 200W, Veeco Probes, CA)

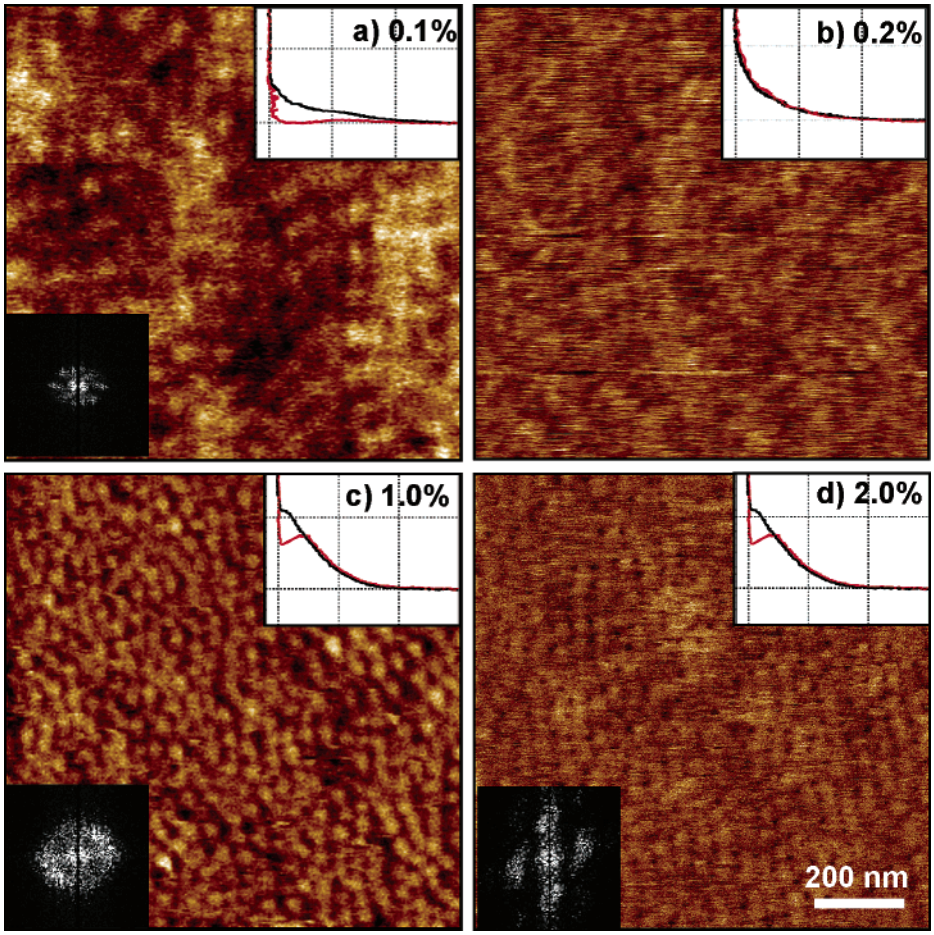

Figure 1. Tapping mode AFM topography images of micelles of $P_{94}E_{316}$ adsorbed onto silica from aqueous solution at concentrations (a) 0.1, (b) 0.2, (c) 1.0, and (d) 2.0 wt %. Height scale is (a) 3.5 nm and (b−d) 7 nm. Insets top right are representative force curves on each surface, corrected to true force−distance. The extension scale of each is −2 to +30 nm, and the force scale is −0.5 to +1.5 nN. Black lines are for tip approach and red lines for tip retraction. The insets bottom left are fast Fourier transforms of the AFM images, all to the same scale.

were cleaned with an O_2 plasma. Thermally equilibrated polymer solution (500 μL, 23 ± 1 °C) was injected into and through the cell, and imaging was performed in fluid tapping mode at a frequency of 8 ± 1 kHz (unless stated—comparison with 30 ± 3 kHz was also made). Imaging or force curve acquisition commenced within 30 s of polymer injection. Interaction forces were minimized by obtaining amplitude/phase-distance curves during scanning. No images could be obtained in contact mode due to sweeping by the tip of weakly adsorbed neutral polymer micelles. Topographical height mode and phase contrast images were acquired simultaneously and are presented with a simple line flattening only.

Micelle densities were measured using the particle analysis function in version 5.12 of the Veeco Nanoscope software. Prior to this analysis, careful background leveling was performed using thresholding to discard high levels and then smoothing with a 3 × 3 pixel Median filter to eliminate spurious pixels that would confuse the analysis. In cases where discrete micelles could not be separated and counted individually, the surface area coverage was measured using the bearing analysis function, with prior image leveling only.

Trajectories of micelle motion were obtained by analyzing successive AFM image frames for the same area of a 1% polymer solution in water adsorbed onto mica. Images were imported into sequential pages of Microsoft Powerpoint at a scale of 40 mm to 100 nm, and the stack of images were aligned to compensate for a small drift between scans. This was made possible by the location of a few small immobile species on the surface (possibly particulate contamination) to use as anchor points. The distance between each micelle could then be measured directly in Powerpoint by measuring the lines drawn between the center of each micelle.

3. Results and Discussion

We studied adsorption onto two substrates, with differing hydrophobicities. The silica used was a silicon wafer with a surface perpendicular to ⟨111⟩ (Prolog Semicor, Kiev, Ukraine), with a 90 nm oxide layer grown at 1100 °C.[39] The heat treatment drives off water from surface silanol groups, leaving behind the more hydrophobic siloxane units,[40] producing a relatively hydrophobic surface with a static water contact angle of 54°.[41] In comparison, mica is more hydrophilic (water contact angle <10° for freshly cleaved mica[42] as used in this study). It is also negatively charged at neutral pH, although that is not relevant to our study of adsorption by nonionic block copolymers. The hydrophilicity of the AFM tip has to be considered also—a contact angle of <5° has been measured for silicon nitride,[43] relatively similar to the value for mica. Cleaning of the silicon nitride tip in an oxygen plasma helps to maintain the hydrophilic character of the silicon nitride and hence the reproducible nature of our results. This property is thought to be due to a thin layer of silicon oxide at the surface.[43]

Adsorption onto Silica. The structure at the silica surface for four different concentrations of $P_{94}E_{316}$ is shown in Figure 1. For the 0.1 wt % sample (below the bulk cmc = 0.23 wt %) the image is composed of fairly regular 45−50 nm diameter (full width half-height) circular features that have a periodicity, or nearest-

neighbor spacing, of 70−90 nm as determined by fast Fourier transform (FFT) processing[37] (Figure 1a). However, these surface humps do not possess clearly defined boundaries, but a smooth undulating transition from one to another. There is some local order at around 400 nm (also shown in the FFT inset), although this does not seem to be as a result of close packing. Phase images[37] at 0.1% on silica show no discernible contrast, indicating a homogeneous surface with a lack of substructure.

If the polymer concentration above this polymer surface is subsequently increased (0.2 to 2.0 wt %), little change is observed, except for indistinct large aggregates which float around from image to image. This indicates that once the initial rapid adsorption process has completed, further adsorption processes are slowed down or halted.

Upon injection of 0.2 wt % polymer (close to the cmc) onto clean silica, a very irregular patchy layer of circular aggregates adsorbs to the surface (Figure 1b). However, images at this concentration proved difficult to obtain; hence the relatively noisy image. The reason for this instability is discussed below. Following injection of the 1 wt % solution onto a clean silica substrate, a monolayer of circular aggregates adsorbs to the surface within the few minutes it takes to complete the first scan (Figure 1c). Upon injection of a 2 wt % solution, again onto a fresh substrate, these pack into a regular, dense array (Figure 1d), with very weakly adsorbed secondary layers beginning to form. The formation of surface micelles between 0.5 and 1 wt % indicates that these form just above the bulk cmc.[38] The formation of surface micelles by EPE triblocks[23,24] and related poly(ethylene oxide)-containing copolymers[24] adsorbed on silica surfaces has been reported previously on the basis of ellipsometry and reflectivity measurements, although to our knowledge images of these micelles have not been presented. AFM has revealed surface micelles for related nonionic C_nE_m surfactants (C = methylene) on hydrophilic silica but not on hydrophobized (via grafted self-assembled monolyers) silica.[25] It has been proposed that E is adsorbed onto hydrophilic silica due to interactions between the O atom in E and −OH groups at the silica surface.[25] A correlation between the formation of surface aggregates and the bulk cmc has previously been noted from adsorption measurements on an EPE triblock, the surface aggregates forming just below the bulk cmc.[24]

The insets in Figure 1c,d show the Fourier transform of images of the micelle layers adsorbed from 1 and 2 wt % solutions. The transform of the 1 wt % topography image shows a random ordering of micelles at a nearest-neighbor separation of 47 ± 3 nm. Because of the presence of very loosely adsorbed secondary aggregates of micelles at 2%, there was some difficulty in observing the packing in the adsorbed monolayer. With a slight increase in tapping force (a lowering of the set point to 90% of the typical scanning set point), a clearer view of the packing could be obtained. This confirms a distorted square packing of micelles, although the distortion results from thermal drift of the scan area over the typical scan time of 3−4 min. From the location of the maxima, the separation between micelles is found to be 39 ± 1 nm. This corresponds very closely to the diameter of bulk micelles, the thermodynamic diameter being 34 nm and the hydrodynamic diameter being 42 nm at 25 °C.[38] This suggests that the regular order results from close packing of micelles, although as we can see later, the ordering/packing process is enhanced by the scanning process itself.

The measured diameter of the surface micelles in the 1 wt % solution is 33 ± 2 nm (with a nearest-neighbor distance of 47 nm), measuring those micelles that have some clear space around them. It is likely that the outer edges of the micelle corona provide a very low force gradient for the tip to detect and will therefore be compressed to some extent before there is enough steric repulsion in the micelle closer to the core. This will result in a measured width smaller than the actual hydrodynamic radius. The measured height is 3 ± 0.2 nm, although this figure is unreliable due to the profile of the AFM tip and the unknown density of invisible adsorbed monomers on the surface between the micelles. It is unlikely that the tip is in contact with the silica substrate even at the lowest point in the image.

Force−distance measurements were also performed on each of these adsorbed polymer surfaces during the imaging experiments to probe the surface architecture. Representative single curves are shown in the insets to Figure 1 and are fully corrected from *z*-piezo extension vs deflection to true force−distance curves. The analysis of these curves is fully described in a previous paper,[37] but a summary of the findings is as follows. The curves at every concentration show a detectable force gradient approximately 20 nm from the final surface ($z = 0$ at high force > 20 nN), in comparison to a typical force curve on clean silica. (Figure 10a is a force curve on mica in pure water, which is identical.) This must be attributable to a steric repulsion as the polymer is neutral. At 0.1 wt % following the initial repulsion the tip moves quite easily to the surface, where it stays upon retract, only moving off the surface when the force is zero. In contrast, at 0.2 wt % the repulsion exhibits a more exponential increase as the tip approaches the surface, characteristic of an end-grafted polymer brush being compressed. There is no hysteresis in the retract curve, indicating the polymer brush is decompressing in the reverse direction. Force curves at 1.0 and 2.0 wt % differ in that the repulsive force initially rises more steeply and becomes almost linear within 8 nm of the surface. This springlike behavior is at odds with the expected exponential brushlike compression and is probably indicative of a structure on the surface undergoing compression. At an applied force of approximately 1 nN the AFM tip suddenly jumps to the incompressible silica surface over a distance of 2−3 nm. This linear compression followed by the tip jump to the surface is attributed to compression of a discrete micelle followed by penetration to the surface or lateral movement of the micelle or tip so that the tip suddenly pushes through to the silica. The displacement of the polymer under compression is analogous to a so-called "escape transition" where at a certain compression part of a chain escapes to avoid the entropic penalty of a highly compact conformation.[44] Escape transitions can occur if the radius of the compressing surface is greater than the dimensions of the polymer coil, but still smaller than its extended length.[44] The escape transition has been modeled by Leermakers[45] in terms of the adsorption parameter of the relevant surfaces (i.e., attractive or repulsive) and the conformational transitions the confined polymer chain undergoes and by Milchev[46] in terms of polymer chain length and piston (probe) geometry. Of particular relevance is the work of Sevick and Williams, who discuss AFM and whose modeled transitions closely

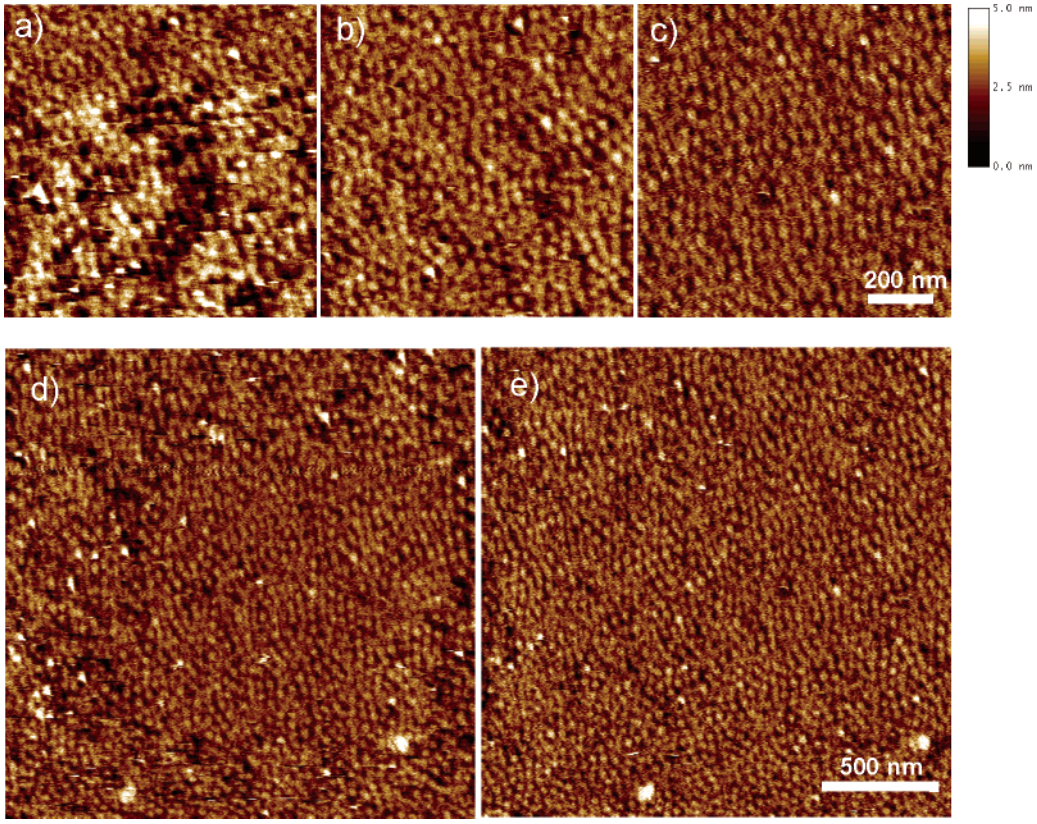

Figure 2. AFM topography images of micelles of $P_{94}E_{316}$ (adsorbed from a 1 wt % solution) on silica. Images a−c show successive scans of the same area. Image d is a zoom out scan with twice the area. The initially scanned region can be seen as the central region of more highly ordered micelles. Image e is a second scan over the same area, showing the ordering of micelles in the previously disordered outer region.

resemble those found in this study.[44] These authors found the profile of the force vs height (or compression) curve to be highly dependent upon the radius, R, of the impacting probe in relation to the size of the tethered monomer. A transition with a similar profile to ours was found when R was between 4 and 5 times the natural size of the chain ($\sqrt{N}$). However, our surface is complicated by the presence of surface aggregates or micelles, hindering quantitative comparison.

On retraction, that contact with silica is made is suggested by the fact that the tip stays in contact with the silica as the positive pressure on the tip is relaxed about 400 pN beyond the point where it broke through. A lateral restorative pressure then pushes the tip away from the surface when the cantilever force is still positive, expelling the tip from the polymer layer. Thereafter, the polymer decompression curve exactly follows the approach curve.

The interaction between the AFM tip and the adsorbed micelles was studied by performing repeated scans over the same area. Figure 2 presents topography images for a 1 wt % solution obtained from successive scans of the same area (approximately 5 min interval between start of collection of each image). The ordering of the micelles develops with repeated scanning. This is best shown by the images in Figure 2d,e. Figure 2d shows a "zoom-out" image obtained by scanning over a larger area that includes the 1 μm × 1 μm initial scan area in the center. The enhanced order of the micelles in this region is evident. A subsequent 2 μm × 2 μm (Figure 2e) scan shows the enhanced packing of micelles as the tip induces ordering of the outer disordered region in Figure 2d. The fact that the micelles outside the scan area do not develop a high degree of order prior to being imaged indicates that the phenomenon is not the result of time-dependent deposition of further polymer or micelles but is brought about by the interaction of the tip with the micelles. A similar effect was observed for micelles deposited onto mica, although as discussed in the following section, the interaction between the tip and polymer molecules was larger since adsorption onto mica was found to be weaker.

Adsorption onto Mica. The adsorption of $P_{94}E_{316}$ onto a hydrophilic substrate, mica, was also investigated. No features, micellar or otherwise, could be discerned on mica at concentrations of 0.5 wt % or below (at a tapping frequency of 8 kHz, see below for data obtained at higher tapping frequencies). The deposition of intact micelles onto a mica substrate from a 1.0 wt % polymer solution was observed by repeatedly scanning the same area by the AFM tip. Figure 3a−c shows selective images from the series obtained. Micelles seem to adsorb onto the Si_3N_4 AFM tip, which has a hydrophilicity similar to mica (as mentioned earlier), and only by successively scanning the same area is the transfer of micelles onto the equally hydrophilic substrate observed. Evidence that intact micelles are transferred from the tip (rather than unassociated polymer chains) is provided by the linear increase in micelle number density with scan time, shown in Figure 4 (time points a−d correspond to the images in Figure 3). Repeatedly scanning in the same area, the number of micelles of uniform size increases steadily. After time point d, the scan area is doubled, to cover the previously scanned region plus unscanned regions around the periphery. It is clear that the number density of micelles is much

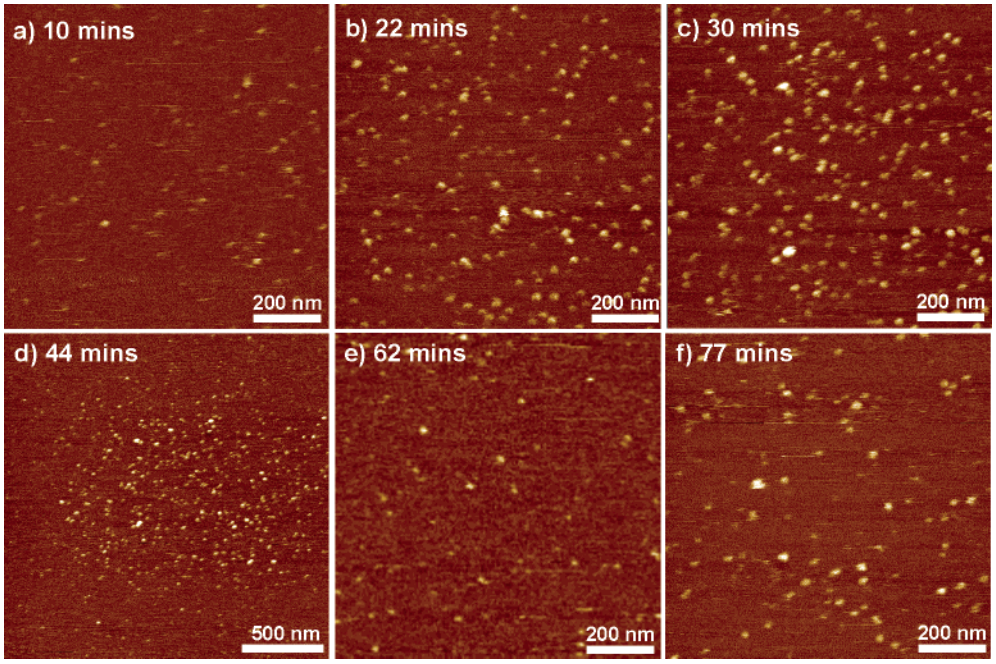

Figure 3. AFM topography images collected from a sequence of successive scans in the same area during deposition of polymer from a 1 wt % solution of $P_{94}E_{316}$ onto mica. The time elapsed since the start of the first scan is indicated. Parts a−c are all 1 μm × 1 μm scans. Image d is a zoom out to a larger 2 μm scan that covers the previously scanned area. The enhanced deposition within the repeatedly scanned region in the center is evident. The sample was then translated so that a fresh area of mica was scanned, image e, and a further sequence of images in the same area was acquired. The deposition of micelles started from the same initial density (approximately 60 micelles per μm^2; see Figure 4) as for the first scan series starting at (a), followed by a linear increase in micelle density proportional to the duration of scanning (f).

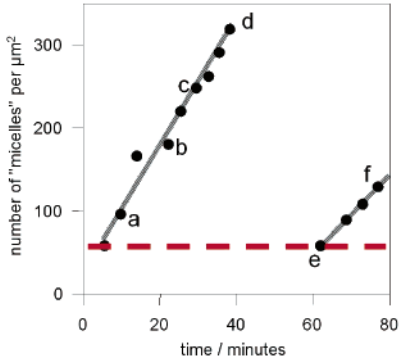

Figure 4. Number of micelles per μm^2 obtained from particle analysis of sequential AFM images during deposition of polymer from a 1 wt % solution of $P_{94}E_{316}$ onto mica, several images of which are shown in Figure 3. Labels a−f on the graph denotes the corresponding image in Figure 3a−f. The scan area is translated between scans labeled d and e; time point e (cf. Figure 3e) is the first scan in a fresh previously unscanned area. The horizontal dashed line indicates the "steady-state" micelle number density outside the area scanned by the AFM tip. Micelle density increases proportionally with time/number of scans, in the scan area only.

higher in the previously scanned area. Enhanced deposition is also precisely within the previous scan area—if the rate of deposition was due to an increase in micelle diffusion brought about by agitation from the oscillating probe, the increase in adsorption might be expected to extend some distance from the scan region. The probe is then translated onto a fresh area of mica where the number density of micelles is the same as that prior to scanning the previous area (horizontal red line in Figure 4). A linear increase in number density during repeated scans is again observed. Time points e and f in Figure 4 relate to the images in Figure 3e,f. The slope of the line is slightly different to the first run which may be due to changes in conditions such as tapping strength, amplitude, or possibly a small change in temperature. We are unsure of the precise origin of this effect at present. Nevertheless, these experiments provide clear information that the rate of deposition of micelles without the AFM tip is rather slow; in fact, a steady-state density of around 60 micelles per μm^2 appears to have been reached. We suppose that micelles in solution attach to the AFM tip due to adsorption of the hydrophilic E block[23] and are steadily transferred by being pushed against the equally hydrophilic mica substrate. The AFM tip is acting as an oscillating nanoscale probe for deposition of nanoscale (micellar) features.

Further evidence of the weak adsorption of micelles on mica is provided by data for a 2 wt % solution, as shown in Figure 5. Although a dense layer of discrete polymer micelles can be observed that have identical dimensions as those seen on silica, the density is less than that seen on silica from a 1 wt % polymer solution and is less regular. In addition, the dark trails, or streaks, evident in the phase contrast image of Figure 5a arise from motion of micelles induced by the tip. As discussed in our previous note,[37] dark contrast corresponds to regions of high energy loss (and hence greater phase lag) due to the tip penetrating the void between adjacent micelles. As phase contrast is very sensitive to the presence of a micelle as opposed to a uniform tethered polymer brush, the dark trails moving together from bottom left to top right indicates micelles being pushed along in the "trace" scan direction (left to right) and the slow scan direction, bottom to top. Linear trails in AFM images that change with scan direction are indicative of very loosely bound species that are nudged along by the tip from scan line to scan line. This effect was not observed for lower polymer concentrations, and we believe it is due to adsorption of a large number of micelles onto the tip during the scan. It leads to changes in the relative separation between, and interaction of,

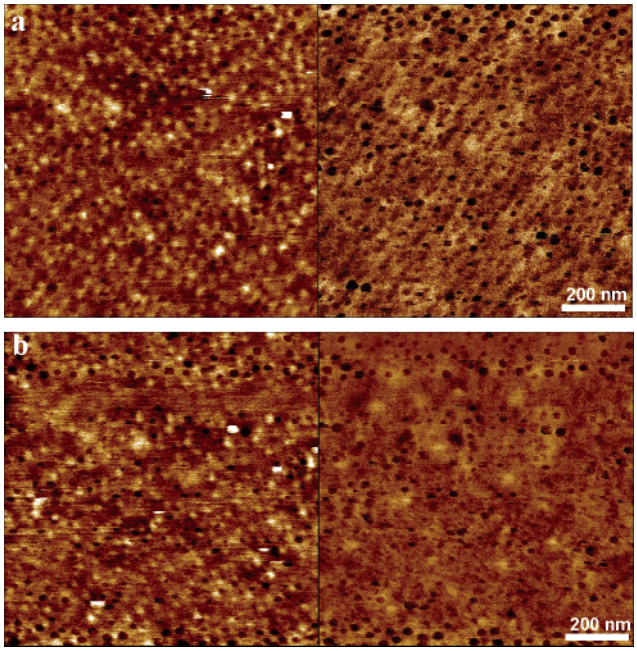

Figure 5. AFM images showing micelles adsorbed from a 2 wt % solution of $P_{94}E_{316}$ adsorbed onto mica. Images from different areas on the same sample are shown in parts a and b. Topography images are on the left, and phase contrast images are on the right.

the tip and the surface. This does not occur at 1.0 wt % polymer because the micelle concentration is relatively low, and any micelles adsorbing to the tip are transferred during tapping onto the relatively clean mica surface (as described above), thereby maintaining image quality and low tip−sample interaction. This might also explain why an increased imaging force was required to obtain a clear image of micelles on silica adsorbed from a 2% polymer solution. In this case the micelles were well adsorbed (and hence immobile), but the large number of micelles adsorbing to the tip interfered with the imaging process; this could only be overcome by deliberately increasing the scanning force so that the micelles are dislodged from the tip, or at least pushed away from the tip apex. This tip force increase was insufficient to move the micelles on silica because on this substrate micelles have completely relaxed into hemispheres with the hydrophobic core in contact with, and strongly adsorbed to, the relatively hydrophobic surface.

Micelles deposited from more dilute solutions were able to move independently. Figure 6 shows three selected frames from a longer sequence (see animation, Supporting Information) that illustrates Brownian-like motion of micelles in a 1 wt % solution on mica. The motion of the micelles contrasts strongly with micelles adsorbed onto silica, which were not mobile. It is consistent with a much weaker interaction between the micelle and mica, as noted from the deposition of micelles by the AFM tip just discussed. This contrasts, for example, with the micelles studied by Webber et al., where electrostatic interactions between the diblock polyelectrolyte and the charged mica lead to strong adsorption.[20] The trajectory of a series of micelles deposited onto mica from a 1% solution is shown in Figure 6d. When the sequence of images is animated (see Supporting Information), it is clear that the same micelles are migrating slowly (and randomly) across the surface, and each AFM image is a snapshot of this motion. The micelles are not dispersing and re-forming in random positions. On the scale of the image, the micelles do not move very far from their initial position. However, they do move a measurable distance in a random walk. New micelles are also alighting on the surface adding to the numbers during the sequence. One micelle is picked up by the tip, dragged across the surface, and broken up, and the evidence of this in the AFM image is a noisy scan line streak starting at the exact position the micelle existed in the previous scan. This is indicated by the long dashed line in Figure 6d. Two smaller fragments appear at the end of the scan-line streak, which then go on to migrate independently in the subsequent images. The other micelles undergo motion that is not related to the direction of the scan. The micelle motion was analyzed to provide root-mean-square displacements. Considering only micelles that remain within the imaging area for the duration (a total of 20 micelles were measured; some micelles adsorb during the scan, with a few micelles desorbing), the rms displacement of individual micelles was obtained, and the mean for all micelles is 23 ± 11 nm (taking the rms value of the displacements of all micelles yields a similar value). The total measurement time, t, was 2900 s. The Brownian motion of the micelles appears to be two-dimensional because there is little evidence for apparent changes in micelle dimensions due to vertical motion. Therefore, we have to modify the usual expression for three-dimensional motion, $\langle r^2 \rangle = 6Dt$. In two dimensions, the corresponding expression becomes $\langle r^2 \rangle = 4Dt$ (using the derivation provided in ref 47). This yields $D = 5 \times 10^{-2}$ nm^2 s^{-1} $= 5 \times 10^{-20}$ m^2 s^{-1}. This is much lower than a typical bulk diffusion coefficient for block copolymer micelles. For $P_{94}E_{316}$ specifically, the bulk diffusion coefficient corresponding to the measured hydrodynamic radius $r_h = 20$ nm (40 °C)[38] is 1×10^{-11} m^2 s^{-1}. The enormous reduction in motion for the micelles adsorbed at the surface points to the adsorption energy associated with this (expected to be $\sim k_B T$).

Experiments were also performed at lower concentrations to study sequential adsorption. It must be noted that the following images were obtained at a tapping frequency of 30 kHz, used in an attempt to define some very vague shifting features observed at the normal 8 kHz imaging frequency. This method is discussed further below. An image of an adsorbed film deposited from a 0.5% solution is shown in Figure 7a. The aggregates are very irregular in shape and smaller than the micelles formed at higher concentration (i.e., from 1% or 2% solutions), the maximum diameter being 10 nm. We believe that these structures are not complete micelles—they can be interpreted as small aggregates of unimers or "premicelles". Adsorption of a 2% solution onto the polymer layer adsorbed from the 0.5% solution was then studied (dashed line in the surface area coverage plot, Figure 7b). A rapid increase in the surface area coverage was observed. The corresponding image of the adsorbed film is shown in Figure 7c. The average size of the aggregates increased slightly, and the surface area covered tripled, although there was no evidence for the formation of complete micelles. This increase in adsorption then leveled off again, indicating that the adsorbed aggregates are in an equilibrium situation with the polymer in solution, and by increasing the polymer concentration, the surface coverage increases to a higher, but constant, level.

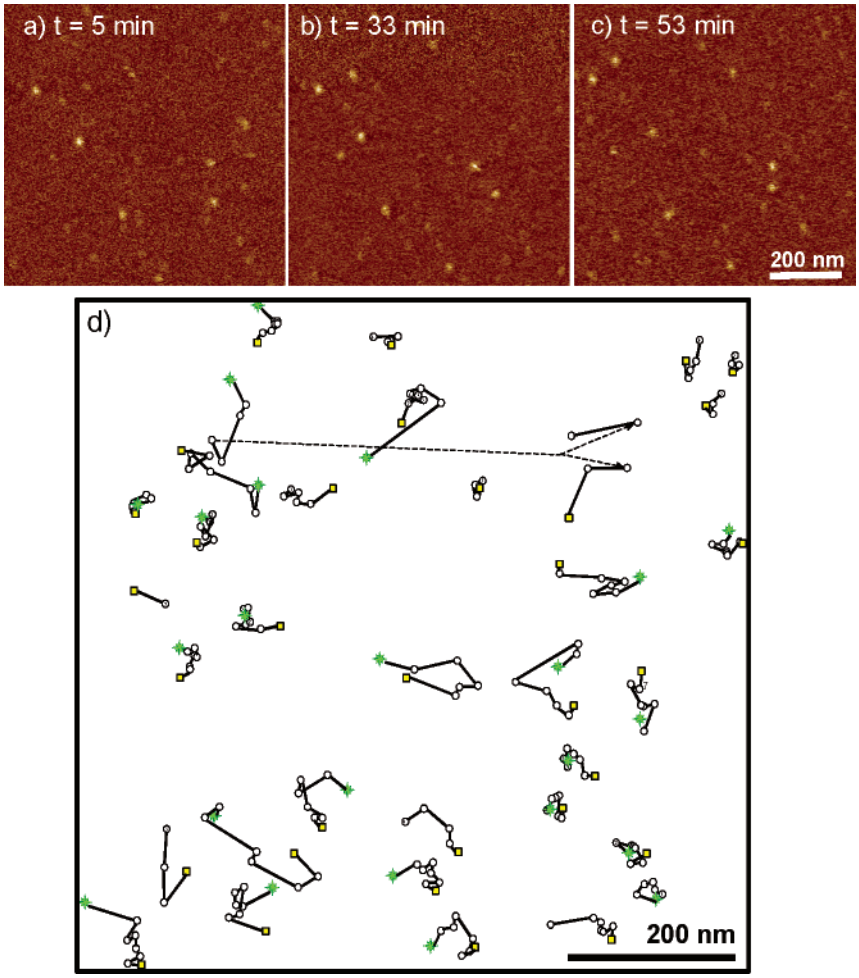

Figure 6. AFM topography images of micelles from a 1 wt % solution of $P_{94}E_{316}$ adsorbed on mica obtained from successive scans of the same area. Part d shows the trajectory of particles over a series of such images. Green crosses indicate the start position (for micelles that were present in the first image of the sequence), and yellow squares indicate final position (for those micelles that remained in the scan area). The dashed line indicates a micelle that was picked up the AFM tip and translated across the surface.

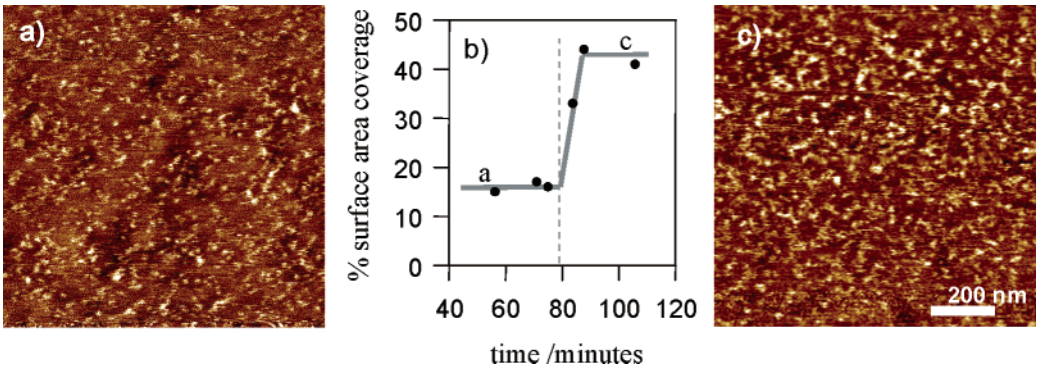

Figure 7. AFM (topographic) images following adsorption on mica from (a) a 0.5 wt % solution, followed by (c) a 2 wt % solution. Part b shows the increase in surface area coverage upon adding the 2 wt % polymer solution. The points at which images a and c were acquired are indicated. Images were acquired at a tip oscillation frequency of 30 kHz.

Block copolymer micelles are soft objects. Therefore, it can be expected that the oscillation frequency of the AFM tip might influence the images, since the viscoelastic response will change. In other words, the image may depend on the high-frequency rheological properties. Figure 8 compares data obtained for 1 wt % solutions on mica at a tip frequency of 8 kHz (Figure 8a) and 30 kHz (Figure 8b). At 8 kHz the micelles have a diameter of 31 nm and a height of 3−4 nm. In contrast, at 30 kHz the micelles have a diameter of 18 nm and a height of 8 nm.

In general, when probed at higher frequencies, soft materials appear stiffer, i.e., have a lower energy loss. The images in Figure 8 are consistent with this, since at higher frequency the micellar features observed are higher and narrower, suggesting a greater resistance to deformation by the tip (Figure 8b). In addition, Figure 8c shows the phase contrast obtained on micelles at low and high frequency. At 8 kHz, a higher energy loss (darker phase contrast) is observed, and there is greater interaction between the tip and micelle, resulting in an image of a flattened pancake-like micelle. At 30 kHz,

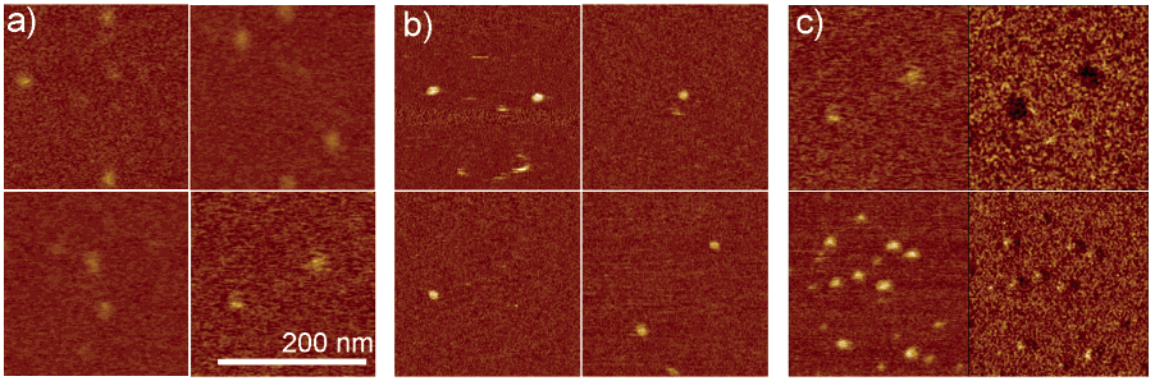

Figure 8. AFM images of micelles adsorbed onto mica from a 1 wt % solution obtained for different tip oscillation frequencies. Images: (a) four topographic images recorded at a tapping frequency of 8 kHz, (b) four topographic images recorded on the same surface at a fluid tapping frequency of 30 kHz, and (c) upper pair of images at 8 kHz and lower pair of images at 30 kHz. In each pair, topography images are on the left and phase contrast images are on the right.

the phase contrast of the micelles in the image shows a shaded appearance typical of hard bodies as though there were no material contrast on the surface, with a bright left-hand edge and dark right-hand edge (Figure 8c). It is known in high-frequency rheology of polymer solutions that the viscoelastic response (storage and loss moduli) changes with frequency. This is due to the particular time scales of the various modes of polymer chain motion. However, further more detailed rheological analysis is required to gain more quantitative information.

At lower concentrations, where well-defined micelles have not formed, the effect of tip oscillation frequency is even more pronounced, as exemplified by Figure 9. This shows an image obtained at 8 kHz following adsorption from a 0.5% solution (Figure 9a). The image is not uniform, and there appear to be some poorly defined features. The tip oscillation frequency was increased to 30 kHz, and a larger area was scanned, encompassing that already scanned at 8 kHz. The topography image obtained is shown in Figure 9b. Adsorbed premicellar aggregate features can now be discerned. The most marked features however are the broad smeared out bands in the center in the region previously scanned. The adsorbed micelle features are not well-defined in this region. This indicates severe disruption of the adsorbed structure at the lower tip frequency. It appears that to image low-density features, a high tip scanning frequency is required to prevent dynamic deformation and sweeping of the aggregates. For this reason, the images presented in Figure 7 were recorded at 30 kHz.

To study the nanomechanics of the adsorbed layer, the tip was used to probe the force as a function of distance from the substrate. Z-piezo extension vs cantilever deflection profiles were recorded throughout the experiment and later converted into true force−distance curves. To obtain quantitative force curves, the spring constant of each cantilever (0.05−0.08 N m^{-1}) was measured using the thermal noise method in air, as described previously.[37] Force−distance curves were studied during adsorption onto mica at 0.5 wt % polymer, during the experiment for which images of the adsorbed structure are shown in Figure 7. Force−distance curves can be acquired much more rapidly (<1 s) than the images (4−6 min for a full scan), and a large series were recorded, of which only selected examples are included in Figure 10.

Figure 10a shows a force−distance profile obtained from pure water, prior to injection of the polymer. Upon

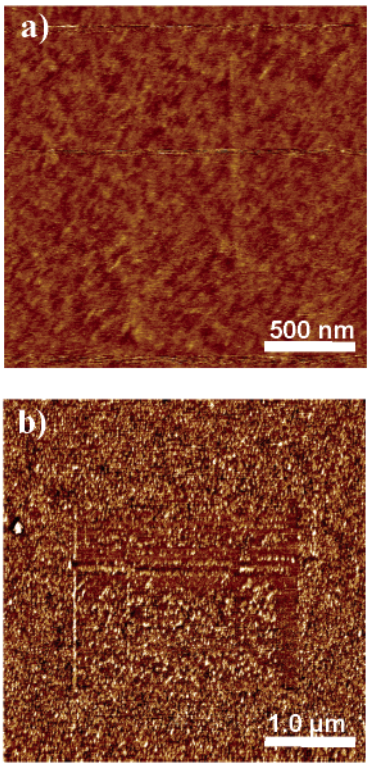

Figure 9. AFM images (topography) highlighting effect of tip oscillation frequency on the resolution of features on an adsorbed layer of aggregates on mica from dilute solution (0.5 wt % $P_{94}E_{316}$). (a) Image at 8 kHz showing poor resolution of features. (b) Image at 30 kHz over a larger area incorporating the region scanned at 8 kHz (center). The effect of the tip at 8 kHz is evident—it severely disrupts the adsorbed aggregates.

approach, repulsion only becomes appreciable at a very small separation (water molecular monolayer adsorbed on mica). Upon retraction, there is substantial hysteresis associated with strong adhesive van der Waals forces. As soon as polymer is adsorbed at the earliest time point (less than 30 s), substantial repulsion of the tip occurred, starting at a tip−sample separation of around 23 nm (Figure 10b). At high force (>20 nN) no penetration of the polymer layer was observed, just a smooth increase in force. Similarly, there was almost no hysteresis on retraction. These features point to adsorption of a dense polymer "brush" layer. For our PE diblock, profiles similar to Figure 10b were obtained for up to 84 s following injection of the polymer. Ultimately, deviations from a smooth increase in repul-

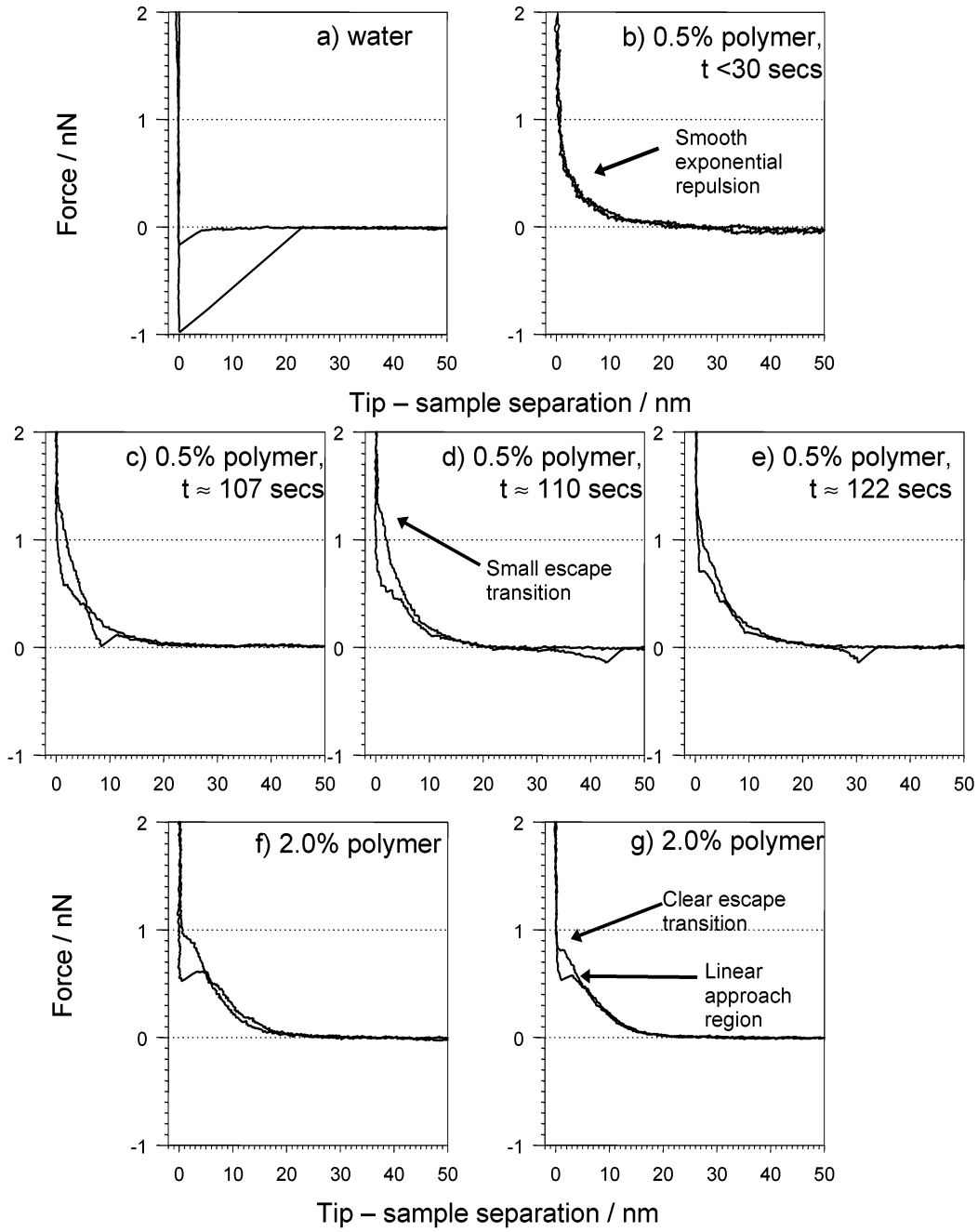

Figure 10. Tip force vs tip−sample separation curves for an experiment monitoring adsorption from a 0.5 wt % solution onto mica: (a) profile for water, prior to injection of polymer; (b−e) profiles obtained following injection of polymer, at the times indicated; (f, g) following injection of a 2 wt % polymer solution onto fresh mica.

sion of the approaching tip are observed at small tip−sample separations (Figure 10c−e). The small jump, or discontinuity, away from the regular exponential approach points to a breakthrough event whereby the tip has encountered greater resistance to penetration of the polymer layer, and the deflection (force) rises more steeply. At about 1 nN applied force this resistance is overcome, and the tip moves quickly to the hard impenetrable substrate. We propose that this is more likely to be due to lateral motion of the aggregate from under the tip, as opposed to a penetration of the polymer layer. As mentioned above, this appears to be an "escape transition". Previously[37] (Figure 1c,d), better resolved examples of this so-called escape transition were shown to occur in force curves acquired on complete micelles adsorbed to silica. However, on mica at low polymer concentration the resistance is very much smaller and almost indistinguishable, reflecting the beginnings of formation of very small surface aggregates. Some small contact with mica is made as the tip remains briefly at the surface as the force on the tip is relaxed.

Purely repulsive forces increasing rapidly with decreasing separation have been observed via experiments using the surface forces apparatus for poly(ethylene oxide)-containing diblock layers adsorbed onto mica from aqueous[48] and nonaqueous[49−51] solvents. However, it must be pointed out that escape transitions are not possible in the surface force apparatus as the surfaces approaching one another are orders of magnitude larger than the species being compressed.[44] The appearance of the escape transition and surface adhesion in the force−distance curve are ascribed to reorganization of the brush layer as surface premicelles begin to form, consistent with the images shown in Figure 7.

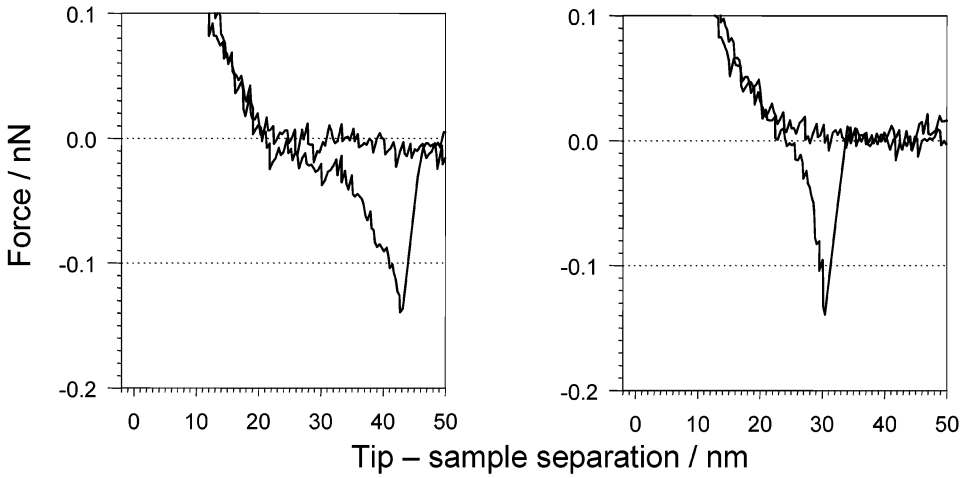

Figure 11. Details of force−distance profiles in Figure 10d,e, showing adhesion and "pull-off" events on retraction. The detachment force is ca. 130 pN.

A very interesting behavior is observed in this regime upon retraction of the tip. As evident from the profiles in Figure 10c−e, strong attractive forces act at certain tip−sample separations. The tip−sample separation at which this is observed varies irregularly within the range 10−50 nm. These features can be associated with adhesion of polymer chains between the tip and the substrate (consistent with the hydrophilic nature of both). Figure 11 contains enlarged portions of the force−distance curves in Figure 10d,e that show this behavior. The detachment force to break these adhesive polymer "bonds" is approximately 130 pN. To our knowledge, AFM has not been used to measure the detachment force for adsorbed block copolymer chains before. The profile of these adhesion events is consistent with a single polymer chain, adsorbed to both tip and substrate. As the tip moves away, the coiled polymer unravels until it is pulled taut, and a negative force on the tip results. This single polymer is then stretched with an increasing nonlinear force that may be described by the wormlike chain model,[52] before one or both ends of the polymer detach from the mica and/or tip in a bond rupture or forced desorption event. Analysis of this chain stretching, although of interest, is beyond the scope of the current paper.

Upon injection of a 2 wt % polymer solution onto fresh mica, we obtained the force−distance profiles shown in Figure 10f,g. These resemble those previously reported by us for the same diblock adsorbed onto silica (Figure 1c,d).[37] Upon approach, the tip again first experiences a steric repulsive force at 20−23 nm, corresponding closely to the bulk hydrodynamic radius. Tip breakthrough events are observed at smaller separations from the surface, as the tip penetrates regions between micelles to contact the surface. This escape transition is more pronounced, cleaner, and entirely repeatable in comparison to the similar events seen for the 0.5 wt % polymer layer, which we ascribed to surface aggregates rather than micelles. There is significant hysteresis associated with this process due to the strong van der Waals forces between the substrate and the tip. Following the sequence shown in Figure 7, force−distance curves were also measured for a 2 wt % solution adsorbing on top of the structure formed from a 0.5 wt % solution. The force−distance curves were similar to those shown in Figure 10 for the 0.5 wt % solution adsorption. This indicates that additional polymer does not significantly influence the formation of the mixed polymer brush/ premicelle aggregate structure. This preexisting layer structure hinders the adsorption of micelles from the 2 wt % solution. Micelles can however adsorb directly onto fresh mica from a 2 wt % solution.

Comparison of Adsorption onto Silica and onto Mica. The adsorbed structure was compared for hydrophilic (mica) and hydrophobic (silica) substrates. Figure 12 shows AFM topography images of surface structures adsorbed from solutions at several concentrations, all obtained at an 8 kHz tapping frequency. In this tapping regime micelles are visible, but surface aggregates are too unstable to resolve. Close to the cmc, the structure adsorbed on the hydrophobic silica substrate is much more ordered than that on mica, although the concentration of polymer was lower in the former case. (We do not have clear data for adsorption onto silica from a 0.5% solution.) The same applies for adsorption from 1% or 2% solutions. At 1% a dense and stable monolayer of discrete micelles is observed on silica, while on mica a relatively small number of micelles are seen that migrate over the surface in a motion seemingly unconnected with the scanning probe. However, rearrangement leading to ordering of micelles, and filling in of gaps on silica, or enhanced deposition on areas of mica continually scanned suggests that in both cases micelles are adsorbing to the hydrophilic Si_3N_4 AFM tip and are then deposited onto the substrate.

For layers adsorbed from 2 wt % polymer solution a very dense layer is observed on both substrates. However, the topographical contrast on silica is low due to the close-packed micellar structure, which prevents the tip penetrating regions in between micelles reducing the height variation of the adsorbed micelle layer. This is reflected in the close-packed ordering of 39 nm as highlighted by the FFT in Figure 1d. On mica, the dense layer of micelles is not ordered and shows evidence of motion induced by the scanning probe (Figure 5). That micelles are adsorbing to the tip in larger numbers at 2% is evidenced by the increased difficulty in obtaining a clear image on both substrates, with the need to substantially increase the imaging force on silica to bring the tip into contact with the strongly adsorbed micelle layer, and the dragging motion of the scanning tip on the micelles more weakly adsorbed to mica.

How can these results be rationalized? In our previous paper[37] on the adsorption of copolymer micelles onto silica, we proposed an adsorption model for that system. Here we extend the model to account for our observa-

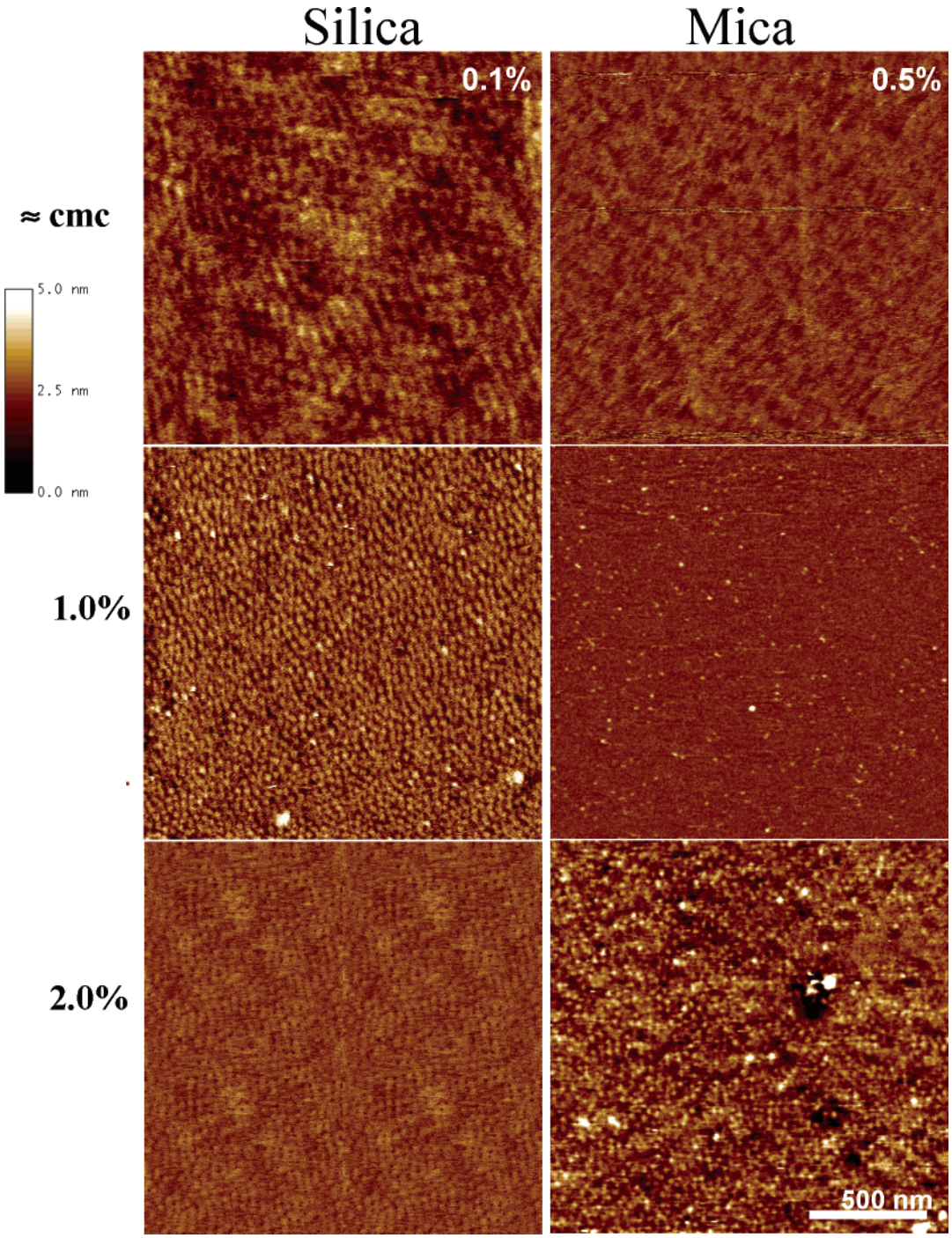

Figure 12. Comparison of adsorption onto silica and mica. AFM topography images at the concentrations indicated. The image for adsorption onto silica from a 2% solution is, for convenience, a composite of smaller images (four 1 μm^2 images) since a 2 μm × 2 μm image was not obtained for this sample.

tions on both substrates. At low concentration (0.1 wt %) below the cmc the block copolymer exists in the solution as unimers (Figure 13). Through physical contact the hydrophobic block will adsorb to the moderately hydrophobic silica. At this low coverage stage a probing AFM tip can meet the surface. As adsorption continues a phase separation occurs, with a concentration of hydrophobic blocks leading to the formation of surface hemimicelles. This process either occurs through preferential adsorption of the hydrophobic block of the unimer from solution into a concentrated pool of previously adsorbed polymer or less likely by the surface mobility of unimer already adsorbed to the silica. The hemimicelles are more diffuse than micelles seen at higher concentration and importantly are structures that form at the surface rather than in solution.

Adsorption of a 0.2 wt % solution (close to the cmc, 0.23 wt % at 20 °C) to clean silica results in force curves indicative of a dense impenetrable end-grafted polymer brush. Conversely, the images, although indistinct, suggest the presence of more spherical micelle-like features. This paradox may be resolved by considering the process of micellization. At this concentration it is beginning, but the few micelles are outnumbered by a much higher concentration of unimers. The probability for micelle adsorption is therefore very low. We propose that individual micelles adsorb, and upon adsorption the micelles relax into a roughly hemispherical structure,

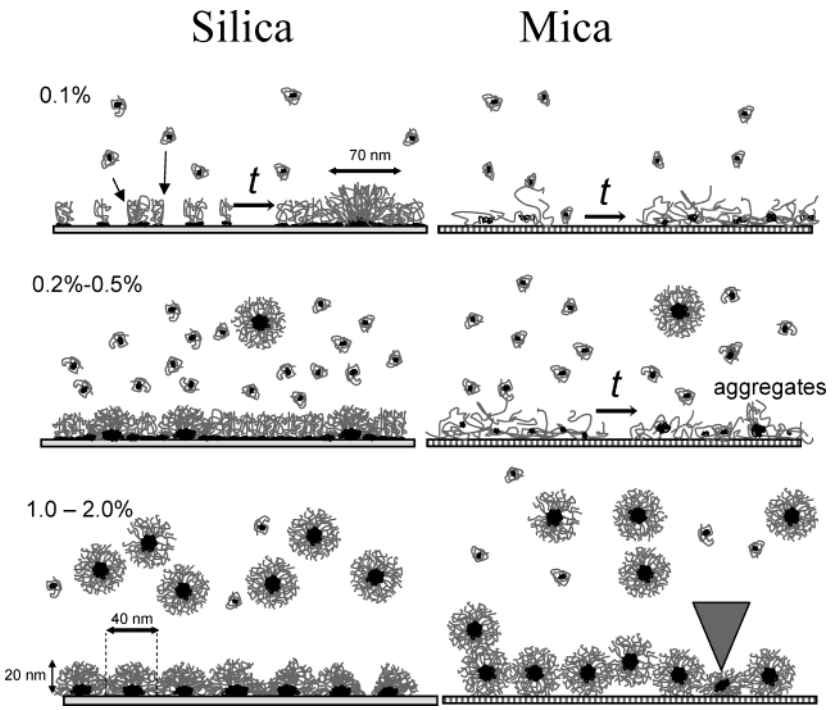

Figure 13. Models for adsorption onto silica and mica at the concentrations indicated. The gray triangle represents the AFM tip.

with the hydrophobic core in contact with the surface. A similar model was put forward by Webber et al. for adsorption of the cationic diblock polyelectrolyte studied by them onto a charged mica surface.[20] The micelles can also be distinguished from the background via their dark phase contrast. However, the unimers are also adsorbing, filling in the gaps where the micelles have not adsorbed. This leads to a mixed surface, which is also fairly unstable to AFM imaging as the micelles are not laterally supported in a close-packed array. It is also possible that unimer adsorption is destabilizing the AFM image by preventing the micelles from fully relaxing onto the surface to increase the contact with the hydrophobic core. When performing a force curve, there is a much higher probability that the tip will contact the quite strongly adsorbed layer of the hydrophobic block, and no breakthrough events are seen.

Adsorption of polymer from low concentration solutions onto mica occurs via a different process (Figure 13). Although we do not have data on mica at concentrations ≤ 0.2%, we have followed the very first stages of adsorption at 0.5%. Upon injection the polymer rapidly forms a repulsive brush-like layer, presumably though adsorption via the hydrophilic E block. At first this forms a uniform blocking tethered monolayer, but as adsorption continues surface aggregates begin to develop after approximately 1.5 min (Figure 10). This is evidenced by small escape transitions followed by direct tip contact with mica. The hydrophobic P blocks have reached a local concentration where they begin to associate. However, adsorption to the substrate is still via the hydrophilic block, and quite weak, so the aggregates are easily swept by the tip, unless the imaging frequency is increased. The aggregate that has formed occupies a space on the surface, and hence when this is pushed aside by the tip (the escape transition), it exposes an area of the surface allowing the tip to contact the mica. At low coverages on mica (before aggregates form) and at low concentrations on silica (where the hydrophobic block of the unimer strongly adsorbs), a uniform brush forms. There is therefore no escape transition, no contact with the substrate, and no tip−substrate adhesion. The aggregates can be observed after a longer time interval by imaging, where the surface coverage appears to have come to an equilibrium. Injection of a higher concentration micelle-containing solution does not lead to micelle adsorption, and the preadsorbed aggregate/unimer brush layer prevents further micellar adsorption. Rather, the equilibrium of aggregates shifts slightly, increasing their size and density to a secondary equilibrium position.

Above the cmc, there is a greater likelihood that micelles will adsorb on both surfaces. For 1.0 wt % polymer on silica the images show a layer of distinct micelles at the surface. At 2.0 wt % these then pack into a denser close-packed array. The force curves on this surface exhibit a different behavior accordingly, with the tip pushing between the micelles in the close-packed layer, through the hydophilic corona between the micelles, and onto the silica surface below. This contact surface is free of adsorbed unimer (which would prevent adhesion) as the micelle as a whole has been pushed aside, exposing clean polymer free substrate. This is a further indication of the integrity and stability of the micelle, despite adsorption and relaxation processes and disturbance by the AFM tip.

The presence of a micelle under the tip is also indicated by the form of the compression curve, with an almost linear springlike response as the spherical micelle is compressed. This is perhaps indicative of core compression, with the corona following an exponential brushlike interaction and the more elastic solid core compressing as a spring. This linear region commences approximately 5−8 nm from the surface (whether mica or silica), suggesting a core diameter of 16 nm, with the first detectable repulsion experienced at 20−23 nm; hence a total micellar diameter of 40−46 nm. 8 nm is also the measured height of isolated micelles on a surface in the high-frequency tapping mode (cf. 3−4 nm at low frequency), suggesting that the AFM is only

imaging the core of the micelle rather than the diffuse corona and that the change in response of the micelle at different frequencies is a measurable change in response of the core only. This interpretation is supported by analysis of SAXS data for micelles in bulk, which provides a core diameter 12−13 nm.[53] The measured width of the core at high frequency is 18 nm, comparable to that implied by the force curves (16 nm). At low frequency the core is more fluid and deformable and is flattened and spread more by the action of the probe. Once the tip is in contact with the silica, it adheres. As the force on the tip is reduced on the retract portion of the force curve cycle, the tip is expelled from the close-packed micelle layer by a restorative lateral pressure due to the strain in the close-packed layer and thereby overcomes the tip−silica adhesion.

Adsorption of micelles to mica above the cmc has a very similar outcome, with dense-packed (although not ordered or close-packed) monolayers. This is clear in the images and in the force curves that contain well-defined escape transitions. However, adsorption is far weaker than to silica, and we propose that the polymer adsorbs to mica via the hydrophilic E block, with the hydrophobic P block staying condensed into aggregates or micellar cores, rather than spreading and relaxing onto the surface. This weaker bonding leads to mobile micelles at concentrations above the cmc, and formation of visible aggregates at concentrations at or below the cmc, rather than the dense end-grafted tethered monolayer observed on silica.

Finally, we are left with the question of why the steric repulsion event on the approach of the force curves (which is similar to the thermodynamic and hydrodynamic radii of the bulk micelles) is identical on mica and silica when we have proposed that the micelles relax onto silica, but not to mica. A possible explanation is that a relaxed micelle will present a corona that is more dense than that of an unrelaxed micelle. When the tip approaches micelles weakly adsorbed to mica, they will compress the corona with almost undetectable force until the force gradient is such that we observe a repulsive deflection, which is likely to be when the density of corona polymer chains is identical to that of the relaxed micelles. This will be at a similar point in the approach curve where the unrelaxed micelles have been compressed to the same density as the relaxed micelle.

We have demonstrated that amphiphilic block copolymers form micelles that adsorb on to solid substrates above the cmc, although via different mechanisms dependent upon the nature of the substrate. In addition unimers, or free chains, absorb below the cmc. These results agree with the simulations of Zhan and Mattice.[31,32] We can also directly confirm the observations of Munch and Gast,[22] who found that the adsorbed amount increases with concentration up to the cmc (aggregate density increases with concentration) and then remains roughly constant, but at a lower level above the cmc (an adsorbed monolayer of micelles). However, Zhan and Mattice also found that at 10 times the cmc (corresponding approximately in our case to a 2.0 wt % solution) adsorption of micelles again exhibited a dependence on concentration, and this might be reflected in our data that indicate loosely adsorbed micelles on top of the first monolayer on silica that resulted in the unstable imaging conditions. There would be a natural tendency for the micelles to repel one another (hence forming the close-packed but discrete micelle monolayer), and micelle adsorption would tend to cease following the first monolayer, until the concentration of micelles was high enough to overcome this barrier. This regime was not observed by Munch and Gast. Further, our results contradict those of Johner and Joanny,[33] who suggest only free chains adsorb, even above the cmc. Tassin et al. postulated that surface adsorbed micelles act as a barrier to subsequent unimer adsorption.[21] If unimers could penetrate between micelles, then following the escape transition it is probable that the tip would experience a polymer surface, rather than a clean substrate, as we find. Our observation of hemispherical surface micelles on silica at concentrations close to the cmc may be compared with the results of optical interferometry studies,[23] where the adsorbed layer was substantially less thick than the hydrodynamic diameter even above the cmc. This points to the presence of relaxed aggregate structures. In agreement with Malmsten et al.,[23] we propose that hydrophobic P adsorbs onto hydrophobic surfaces. The recent work by Brandani and Stroeve[35] also showed an absorption maximum at the cmc, although their substrate was highly hydrophobic. By changing the proportion of hydrophilic and hydrophobic components of their EPE triblock copolymers, they observe different structures at their model surface, i.e., micellar aggregates from a polymer with a higher hydrophobic content and uniform brushlike monolayers from a more hydrophilic copolymer. This could be reconciled with our findings in that their largely hydrophobic micelles absorb and relax onto the highly hydrophobic surface retaining their integrity, while with the mainly hydrophilic micelles, the smaller hydrophobic cores are attracted to the surface as a dense layer, forcing the hydrophilic chains to extend upward forming a monolayer brush.

4. Summary

Tapping mode AFM performed in situ in aqueous solution has been used to probe the adsorbed structure of an amphiphilic diblock on two substrates of differing hydrophobicity. Adsorption onto mica is weak, as evidenced by a number of features, including the micelle motion imaged for a relatively dilute solution and the deposition of micelles observed when successively scanning the same area. The former process was analyzed to provide a two-dimensional diffusion coefficient (5×10^{-20} m^2 s^{-1}) that was orders of magnitude smaller than that in the bulk, reflecting the confinement at the surface. Just above the cmc the density of micelles on mica increased linearly with scan time. There was no evidence of significant deposition of micelles above the steady-state coverage outside the scan area. The deposition of micelles during scanning by the AFM tip was ascribed to initial adsorption onto the hydrophilic silicon nitride AFM tip and subsequent transfer to the surface. This effect was also observed for micelles on silica, although it was less dramatic in this case manifesting itself in a filling in of final vacant sites on the surface and reordering. This was evident from a number of features, including the absence of diffusive micelle motion (as opposed to tip-driven) even in dilute solution and the formation of a more highly ordered structure at a given concentration compared to adsorption onto mica. Surface micelles were formed on silica at around the bulk cmc (0.23 wt %) with a close-packed array forming at 2.0 wt %. On mica, premicellar aggregates were observed at low concentration. Surface micelles

were observed in a 1 wt % solution, although even at 2 wt % these were not close-packed. The diameter of the micelles determined from AFM images (39 ± 1 nm) was close to the bulk hydrodynamic radius (42 nm).

The effect of tip scanning frequency was studied. A high scanning frequency (∼30 kHz) was required to image the loose premicelles adsorbed onto mica from dilute solutions. Low scan frequencies (∼8 kHz) led to significant energy loss as the tip interacted with the adsorbed polymer, leading to disruption of the features. Increasing tapping frequency caused less damping in phase contrast images since the micelles exhibit greater resistance to deformation at high frequency.

Finally, force−distance curves were used to probe the adsorbed polymer layer under varying conditions. In an initial regime (low adsorbed amounts) on both surfaces the repulsive force increases as the tip approaches the substrate, corresponding to repulsion by a dense polymer brush. Little hysteresis is observed as the tip retracts and the layer decompresses. However, as adsorption continues on mica, surface aggregates begin to form as the polymer chains migrate and the hydrophobic P blocks associate. The aggregates are still adsorbed to the mica via the hydrophilic E block. In contrast, on the hydrophobized silica the P blocks adsorb to the surface, acting as a tether, with E blocks forming a dense impenetrable polymer brush. Existence of aggregates and micelles is indicated by a characteristic escape transition in the force curves, with the tip pushing the condensed polymer chains aside exposing clear substrate to which the tip adheres briefly through a van der Waals interaction. At higher concentration, where regular surface micelles are formed, tip breakthrough events are consistently observed at small tip−sample separations. It is proposed that these arise as the tip penetrates between the (now clearly defined) micelles. A linear portion of the approach curve before the transition is indicative of compression of an elastic body rather than a polymer brush. This commences ca. 8 nm from the surface. As 8 nm is also the height of an isolated micelle in a higher tapping frequency image, we interpret this as evidence for interaction with the micelle core.

Acknowledgment. We acknowledge the EPSRC for supporting S.C. (Grant GR/ M51994) and the MRC for supporting S.D.C. (Grant G990 1098). Dr. Connell is also a member of the Astbury Centre for Structural Molecular Biology, University of Leeds.

Supporting Information Available: Animation illustrating Brownian-like motion of micelles in a 1 wt % solution on mica. This material is available free of charge via the Internet at http://pubs.acs.org.

References and Notes

(1) *Surfactant Adsorption and Surface Solubilization*; Sharma, R., Ed.; American Chemical Society: Washington, DC, 1995; Vol. 615.
(2) Edens, M. W.; Whitmarsh, R. H. Applications of Block Copolymer Surfactants. In *Developments in Block Copolymer Science and Technology*; Hamley, I. W., Ed.; Wiley: Chichester, 2004; p 325.
(3) Spatz, J. P.; Roescher, A.; Möller, M. *Adv. Mater.* **1996**, *8*, 337.
(4) Spatz, J. P.; Mössmer, S.; Hartmann, C.; Möller, M.; Herzog, T.; Krieger, M.; Boyen, H.-G.; Ziemann, P.; Kabius, B. *Langmuir* **2000**, *16*, 407.
(5) Spatz, J. P.; Sheiko, S.; Möller, M. *Macromolecules* **1996**, *29*, 3220.
(6) Förster, S.; Hermsdorf, N.; Leube, W.; Schnablegger, H.; Lindner, P.; Böttcher, C. *J. Phys. Chem. B* **1999**, *103*, 6657.
(7) Price, C.; Woods, D. *Eur. Polym. J.* **1973**, *9*, 827.
(8) Booth, C.; Naylor, T. D.; Price, C.; Rajab, N. S.; Stubbersfield, R. B. *J. Chem. Soc., Faraday Trans. 1* **1978**, *74*, 2352.
(9) Zhang, L.; Eisenberg, A. *Science* **1995**, *268*, 1728.
(10) Mortensen, K.; Talmon, Y. *Macromolecules* **1995**, *28*, 8829.
(11) Breulmann, M.; Förster, S.; Antonietti, M. *Macromol. Chem. Phys.* **2000**, *201*, 204.
(12) Gohy, J.-F.; Antoun, S.; Jérôme, R. *Macromolecules* **2001**, *34*, 7435.
(13) Zhu, J.; Eisenberg, A.; Lennox, R. B. *J. Am. Chem. Soc.* **1991**, *113*, 5583.
(14) Zhu, J.; Lennox, R. B.; Eisenberg, A. *J. Phys. Chem.* **1992**, *96*, 6.
(15) Li, S.; Hanley, S.; Khan, I.; Varshney, S. K.; Eisenberg, A.; Lennox, R. B. *Langmuir* **1993**, *9*, 2243.
(16) Zhu, J.; Hanley, S.; Eisenberg, A.; Lennox, R. B. *Makromol. Chem., Macromol. Symp* **1992**, *53*, 211.
(17) Meiners, J. C.; Ritzi, A.; Rafailovich, M. H.; Sokolov, J.; Mlynek, J.; Krausch, G. *Appl. Phys. A: Mater. Sci. Process.* **1995**, *61*, 519.
(18) Regenbrecht, M.; Akari, S.; Förster, S.; Möhwald, H. *J. Phys. Chem. B* **1999**, *103*, 6669.
(19) Webber, G. B.; Wanless, E. J.; Armes, S. P.; Baines, F. L.; Biggs, S. *Langmuir* **2001**, *17*, 5551.
(20) Webber, G. B.; Wanless, E. J.; Bütün, V.; Armes, S. P.; Biggs, S. *Nano Lett.* **2002**, *2*, 1307.
(21) Tassin, J. F.; Siemens, R. L.; Tang, W. T.; Hadziioannou, G.; Swalen, J. D.; Smith, B. A. *J. Phys. Chem.* **1989**, *93*, 2106.
(22) Munch, M. R.; Gast, A. P. *Macromolecules* **1990**, *23*, 2313.
(23) Malmsten, M.; Linse, P.; Cosgrove, T. *Macromolecules* **1992**, *25*, 2474.
(24) Eskilsson, K.; Tiberg, F. *Macromolecules* **1998**, *31*, 5075.
(25) Grant, L. M.; Tiberg, F.; Ducker, W. A. *J. Phys. Chem. B* **1998**, *102*, 4288.
(26) Muller, D.; Malmsten, M.; Tanodekaew, S.; Booth, C. *J. Colloid Interface Sci.* **2000**, *228*, 317.
(27) Muller, D.; Malmsten, M.; Tanodekaew, S.; Booth, C. *J. Colloid Interface Sci.* **2000**, *228*, 326.
(28) Eskilsson, K.; Ninham, B. W.; Tiberg, F.; Yaminsky, V. V. *Langmuir* **1998**, *14*, 7287.
(29) van Lent, B.; Scheutjens, J. H. M. *Macromolecules* **1989**, *22*, 1931.
(30) Evers, O. A.; Scheutjens, J. M. H. M.; Fleer, G. J. *Macromolecules* **1990**, *23*, 5221.
(31) Zhan, Y.; Mattice, W. L. *Macromolecules* **1994**, *27*, 677.
(32) Zhan, Y.; Mattice, W. L. *Macromolecules* **1994**, *27*, 683.
(33) Johner, A.; Joanny, J. F. *Macromolecules* **1990**, *23*, 5299.
(34) Ligoure, C. *Macromolecules* **1991**, *24*, 2968.
(35) Brandani, P.; Stroeve, P. *Macromolecules* **2003**, *36*, 9492.
(36) Brandani, P.; Stroeve, P. *Macromolecules* **2003**, *36*, 9502.
(37) Connell, S. D.; Collins, S.; Yang, Z.; Hamley, I. W. *Langmuir* **2003**, *19*, 10449.
(38) Yang, Z.; Pousia, E.; Heatley, F.; Price, C.; Booth, C.; Castelletto, V.; Hamley, I. W. *Langmuir* **2001**, *17*, 2106.
(39) Collins, S.; Hamley, I. W.; Mykhaylyk, T. A. *Polymer* **2003**, *44*, 2403.
(40) Israelachvili, J. N. *Intermolecular and Surface Forces*; Academic Press: San Diego, 1992.
(41) Mykhaylyk, T. A. University of Leeds, unpublished results, 2004.
(42) Falini, G.; Fermani, S.; Conforti, G.; Ripamonti, A. *Acta Crystallogr.* **2002**, *D58*, 1649.
(43) Tsukruk, V. V.; Bliznyuk, V. N. *Langmuir* **1998**, *14*, 446.
(44) Sevick, E. M.; Williams, D. R. M. *Macromolecules* **1999**, *32*, 6841.
(45) Leermakers, F. A. M.; Gorbunov, A. A. *Macromolecules* **2002**, *35*, 8640.
(46) Milchev, A.; Yamakov, V.; Binder, K. *Phys. Chem. Chem. Phys.* **1999**, *1*, 2083.
(47) Jones, R. A. L. *Soft Condensed Matter*; Oxford University Press: Oxford, 2002.
(48) Schillén, K.; Claesson, P. M.; Malmsten, M.; Linse, P.; Booth, C. *J. Phys. Chem. B* **1997**, *101*, 4238.
(49) Dai, L.; Toprakcioglu, C. *Macromolecules* **1992**, *25*, 6000.
(50) Taunton, H. J.; Toprakcioglu, C.; Fetters, L. J.; Klein, J. *Nature (London)* **1988**, *332*, 712.
(51) Taunton, H. J.; Toprakcioglu, C.; Fetters, L. J.; Klein, J. *Macromolecules* **1990**, *23*, 571.
(52) Best, R. B.; Clarke, J. *Chem. Commun.* **2002**, *3*, 183.
(53) Castelletto, V.; Hamley, I. W., unpublished results, 2004.

MA049396F